JOURNAL OF AGRICULTURAL AND FOOD CHEMISTRY
ARTICLE

J. Agric. Food Chem. 2009, 57, 7331–7337 7331
DOI:10.1021/jf901477g

Magnolol Inhibits Human Glioblastoma Cell Proliferation through Upregulation of p21/Cip1

Li-Ching Chen,[†] Yu-Chi Liu,[∥] Yu-Chih Liang,[‡] Yuan-Soon Ho,[‡] and Wen-Sen Lee*,[†,§,⊥]

[†]Graduate Institute of Medical Sciences, [‡]Department of Biomedical Technology, [§]Department of Physiology, School of Medicine, Taipei Medical University, Taipei, Taiwan, [∥]Department of Ophthalmology, Taipei Veterans General Hospital, Taipei, Taiwan, and [⊥]Cancer Research Center, Taipei Medical University and Hospital, Taipei, Taiwan

Previously, we demonstrated that magnolol isolated from the bark of *Magnolia officinalis* has anticancer activity in colon, hepatoma, and leukemia cell lines. In this study, we show that magnolol concentration dependently (0−40 μM) decreased the cell number in a cultured human glioblastoma cancer cell line (U373) and arrested the cells at the G0/G1 phase of the cell cycle. Magnolol treatment decreased the protein levels of cyclins A and D1 and increased p21/Cip1, but not cyclins B and D3, cyclin-dependent kinase (CDK)2, CDK4, CDC25C, Weel, p27/Kip1, and p53. The CDK2-p21/Cip1 complex was increased, and the CDK2 kinase activity was decreased in the magnolol-treated U373. Pretreatment of U373 with p21/Cip1 specific antisense oligodeoxynucleotide prevented the magnolol-induced increase of p21/Cip1 protein levels and the decrease of DNA synthesis. Magnolol at a concentration of 100 μM induced DNA fragmentation in U373. Our findings suggest the potential applications of magnolol in the treatment of human brain cancers.

KEYWORDS: Magnolol; G0/G1 arrest; p21/Cip1; CDK2; U373 glioblastoma cells

INTRODUCTION

Malignant glioblastomas are the most common primary brain tumor. Despite remarkable advances in surgical techniques and treatment options, including chemotherapy and radiotherapy, the prognosis of malignant glioblastomas is still poor because of their diffuse invasion of the brain parenchyma, which is difficult for total surgical resection (*1*). In fact, the 5 year survival rate for the most malignant type, glioblastoma multiforme, is only 2%. Curative therapy without damaging the affected brain parenchyma is very difficult due to the infiltrative growth patterns and the natural resistance to chemotherapy of malignant glioblastomas (*2*). The standard chemotherapy regimen for patients with oligodendroglioma involves combined treatment with procarbazine, lomustine, and vincristine (*3*, *4*). Each of these drugs was discovered several decades ago with central neurotoxic side effects (*5*−*7*). Obviously, there is an urgent need for new therapeutic strategies in treating malignant glioblastomas.

Magnolol (MAG), a hydroxylated biphenyl compound also known as Hou p'u among Chinese herbalists, has been reported to have anticancer activity (*8*, *9*). Our previous studies demonstrated that MAG suppressed proliferation of cultured human colon and liver cancer cells by inhibiting DNA synthesis and activating apoptosis (*10*). Similar results were also reported by Yang et al. showing that MAG inhibited proliferation of human lung squamous carcinoma CH27 cells at lower concentrations (10−40 μM) and induced apoptosis at higher concentrations (80−100 μM) (*11*). Recent studies demonstrated that MAG could inhibit hepatic metastasis from an experimental liver and spleen metastasis model using L5178Y-ML25 lymphoma and reduce the incidence of pulmonary metastases in the lung metastasis model using B16-BL6 melanoma (*12*). These findings suggest the potential for MAG in cancer chemoprevention. Although the antitumor effects of MAG have been investigated in various cancer cell lines, little is known about its effect on the malignant gliomas of the central nervous system.

Here, we showed that MAG inhibited the proliferation of glioblastoma cells in vitro. These experimental findings reported below highlight the molecular mechanisms of MAG-induced antigrowth activity in U373 cells.

MATERIALS AND METHODS

Cell Lines and Cell Culture. The human astrocytoma cell line, U373, was obtained from the American Type Culture Collection (Rockville, MD) and cultured in 75 cm^2 culture flasks (Greiner, Frickenhausen, Germany). Cells were grown in minimum essential medium with Eagle's salts (MEM; Invitrogen Corp.) containing glutamine (2 mM), 1% nonessential amino acids (NEAA), sodium pyruvate (1 mM), and 10% fetal bovine serum (FBS) in a humidified incubator (37 °C and 5% CO_2).

Reagents. MAG was purchased from Pharmaceutical Industry, Technology and Development Center (Taiwan). Antibodies against cyclin A, cyclin D1, cyclin-dependent kinase 4 (CDK4), CDC25C, Wee1, P21, P53, and CHK1 were purchased from Santa Cruz Biotechnology, Inc. (Santa Cruz, CA). Antibodies against p27 and CDK2 were purchased from BD Bioscience Pharmingen (San Diego, CA). Antibodies against cyclin B and cyclin D3 were purchased from Transduction Laboratories (San Jose, CA). Anti-p-CHK1 antibody was purchased from Cell Signaling Technology,

*To whom correspondence should be addressed. Tel: +886-2-2739-1775. Fax: +886-2-2739-1775. E-mail: wslee@tmu.edu.tw.

Published on Web 08/03/2009

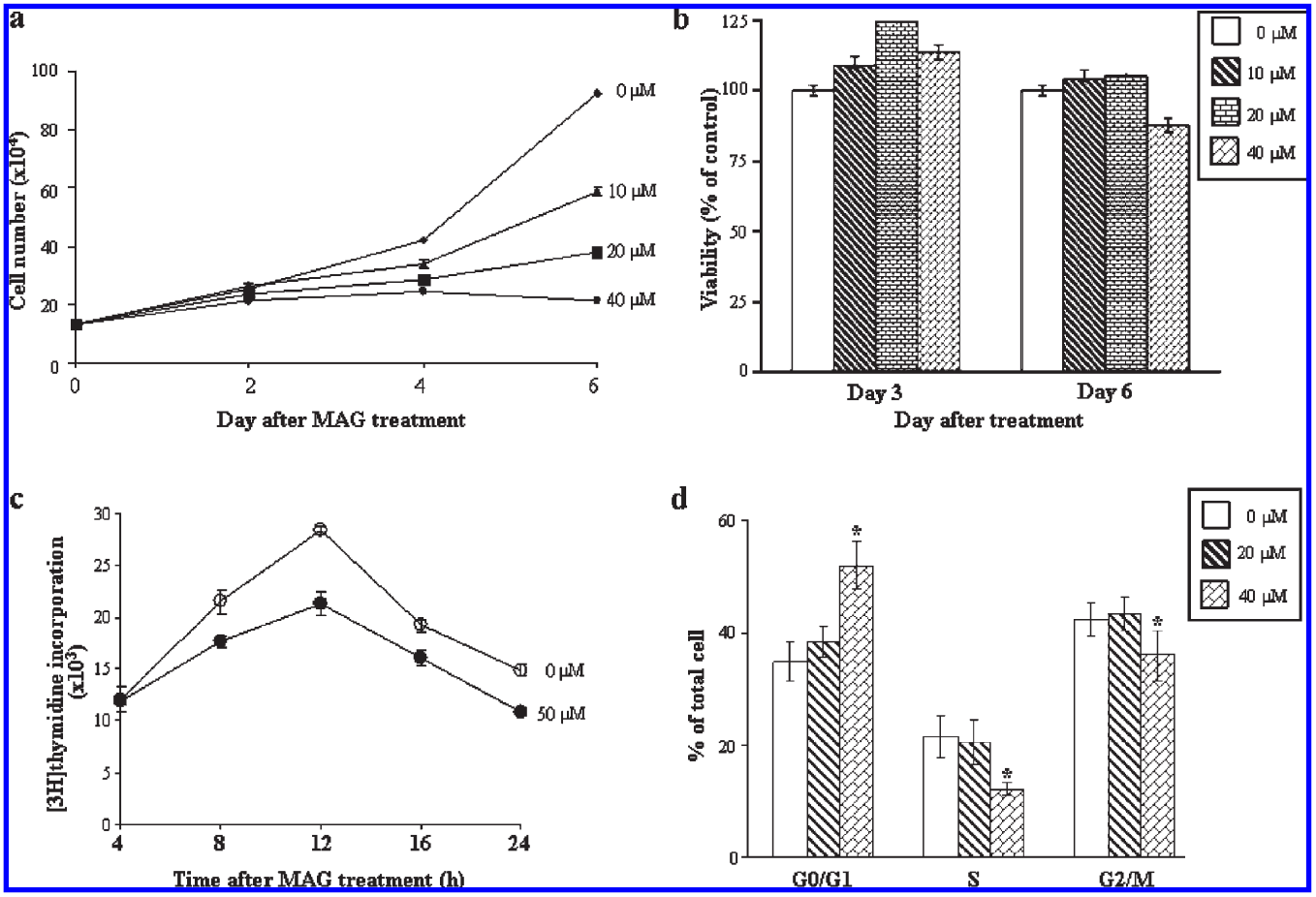

Figure 1. Effects of MAG on cell growth rate in U373. (**a**) MAG (0−40 μM) induced a concentration- and time-dependent inhibition of cell growth in U373 cells. Three samples were analyzed in each group. (**b**) There was no significant difference in viability between vehicle- and MAG-treated U373 cells. (**c**) Time-dependent inhibition of cell cycle by MAG. [^{3}H]thymidine incorporation was conducted after U373 cell release from quiescence by incubation in culture media supplemented with 10% FBS and 0.05% DMSO (control) or 50 μM MAG. (**d**) FACS analysis of DNA content after 18 h of release from quiescence by incubation in culture media supplemented with 10% FBS and DMSO or MAG (20 or 40 μM). The percentage of cells in G0/G1, S, and G2/M phases of the cell cycle was determined using established Cellquest DNA analysis software. Values represent the mean ± SEM (n = 4). *P < 0.05 different from control.

Inc. (Danvers, MA). Anti-G3PDH antibody was purchased from Jackson ImmunoResearch Laboratories Inc. (West Grove, PA).

Determination of Cell Growth Curve. Human U373 (1×10^5) cells were plated in 35 mm Petri dishes and grown in MEM supplemented with 10% FBS. Dimethyl sulfoxide (DMSO), 0.05% (v/v), without (control) or with MAG was added. The incubation medium was changed daily until cell count. The cell number was determined by using the MTT assay.

Trypan Blue Exclusion Assay. As previously described (*13*), cell viability was estimated by the trypan blue exclusion assay at 3 or 6 days after MAG (0−40 μM) treatment. Briefly, human U373 (1×10^5) cells were plated in the 6 cm Petri dishes and grown in MEM supplemented with 10% FBS. The culture medium and MAG were changed daily until the trypan blue exclusion assay.

[^{3}H]Thymidine Incorporation. As previously described (*10*), U373 cells at a density of 1×10^4 cells/cm^3 were plated in 24 well plates and grown in growth medium (MEM plus 10% FBS). After the cells had grown to 70% confluence, they were rendered quiescent by incubation in MEM containing 0.04% FBS for 24 h. The U373 cells were then treated with MAG in MEM supplemented with 10% FBS for the indicated time points. During the last 3 h of the incubation, [^{3}H]thymidine was added at 1 μCi/mL (1 μCi = 37 kBq). Incorporated [^{3}H]thymidine was extracted in 0.2 N NaOH and measured in a liquid scintillation counter.

Flow Cytometric Analysis (*14*). At 24 h after the cells were plated, the medium was removed. Cells were washed three times with PBS and then incubated with medium containing 0.04% FBS for 24 h. After serum starvation, the cells were then challenged with medium containing 10% FBS. The stages of cell cycle were determined by flow cytometic analysis. Cells were incubated with 50 μg/mL propidium iodide (Sigma), and DNA content was measured using a FACSCAN laser flow cytometric analysis system (Becton Dickenson, San Jose, CA). Ten thousand cells were analyzed for each sample.

Western Blot Analysis. Western blot analysis was performed as described previously (*15*). Briefly, cell lysates were prepared, electrotransferred, immunoblotted with antibodies, and then visualized by incubating with the colorigenic substrates [nitro blue tetrazolium (NBT) and 5-bromo-4-chloro-3-indolyl-phosphate (BCIP)] (Kirkegaard & Perry Laboratories, MD). The levels of G3PDH protein were detected and used as the control for equal protein loading.

Immunoprecipitation (IP) and Kinase Activity Assay. As previously described (*16*), the MAG-treated cells were lysed in Rb lysis buffer [137 mM NaCl, 20 mM Tris, pH 7.9, 10 mM NaF, 5 mM EDTA, 1 mM EGTA, 10% (v/v) glycerol, 1% triton X-100, 1 mM sodium orthovanadate, 1 mM sodium pyrophosphate, 100 μM β-glycerophosphate, 1 mM PMSF, 10 μg/mL aprotinin, and 10 μg/mL leupeptin] and immunoprecipitated with anti-CDK2 or anti-CDK4 antibody (2 μg/mL). The protein complexes in beads were washed twice with Rb lysis buffer and then once with Rb kinase assay buffer. The levels of phosphorylated of Rb (for pRb), histone H1 (for CDK2), and glutathione s-transferase-Rb fusion protein (for CDK4) were measured by incubating the beads with 40 μL of hot Rb kinase solution [0.25 μL (2 μg) of Rb-GST fusion protein (Santa Cruz Biotechnology), 0.5 μL of (γ-^{32}P) ATP (Amersham), 0.5 μL of 0.1 mM ATP, and 38.75 μL of Rb kinase buffer] at 37 °C for 30 min and then stopped by boiling the samples in SDS sample buffer for 5 min. The samples were analyzed by 12% SDS-PAGE, and the gel was then dried and subjected to autoradiography.

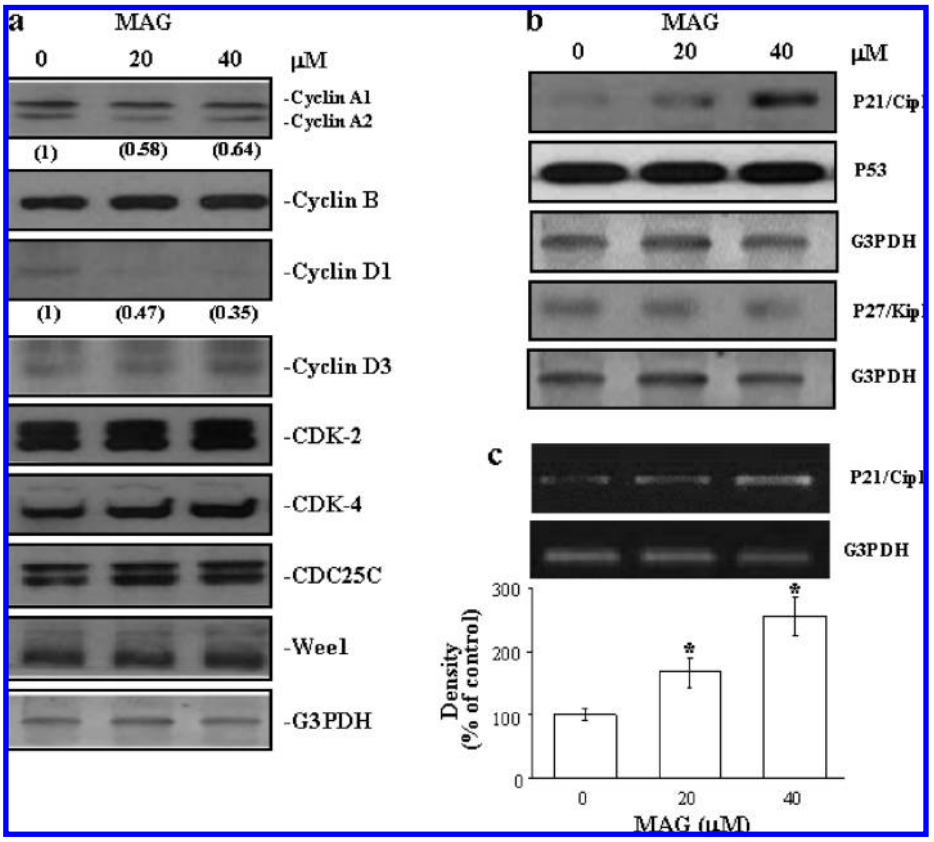

Figure 2. Effect of MAG on the levels of cell cycle regulatory proteins. Proteins were extracted from the cultured U373 cells at 24 h after MAG treatment and probed with proper dilutions of specific antibodies. (**a**) MAG (0−40 μM) concentration dependently decreased the protein levels of cyclins A and D1 but not cyclin B, cyclin D3, CDK2, CDK4, CDC25C, and Wee1. Results from a representative experiment are shown. Values shown in parentheses represent the relative protein abundance of cyclin A and D1. (**b**) MAG increased the protein levels of p21/Cip1 but not p27/Kip1 and p53. The membrane was probed with anti-G3PHD antibody to verify equivalent protein loading. (**c**) MAG concentration dependently increased the levels of p21/Cip1 mRNA. Top panel: A representative measurement of the levels of p21/Cip1 mRNA. Bottom panel: Quantitative results of p21/Cip1 mRNA, which were adjusted with corresponding G3PDH mRNA level and expressed as a percentage of control. Values represent the means ± SEM ($n = 3$). *$P < 0.05$ different from control.

DNA Fragmentation Analysis. The DNA was isolated from U373 cells treated with or without MAG and incubated overnight with nuclease-free proteinase K at 55 °C in 10 mM Tris, pH 7.5, 150 mM EDTA, and 0.5% sodium dodecyl sulfate (SDS). The DNA was then used for detection of DNA laddering as described previously (*15*).

Antisense Oligonucleotide. The p21/Cip1-specific antisense (5′-TCCCCAGCCGGTTCTGACAT-3′) and sense (5′-ACCTGTGCTCCGACACGTCT-3′) phosphothioates were designed as previously described (*17*), synthesized, and purified using high-performance liquid chromatography by Genset. Antisense or sense p21/Cip1 was added to U373 at a final concentration of 20 nM at 16 h before the cell was challenged with 10% FBS and 50 μM MAG treatment for additional 18 h.

Reverse Transcriptase-Polymerase Chain Reaction (RT-PCR) Analysis. The RT-PCR assays for p21/Cip1 gene expression were performed as described previously (*18*, *19*). The U373 cells were treated with MAG for 24 h. Total RNAs were isolated from U373 cells using Trizol reagent according to the manufacturer's protocol (Life Technologies, Inc.). The cDNA was amplified from 1 μg of total RNA using a SuperScript one-step RT-PCR with platinum Taq system (Life Technologies, Inc.). PCR was conducted for 30 cycles in thermal controller. Primers used for amplification were as follows: p21/Cip1 5′-ATTAGCAGCGGAACAAGGA GTCAGACAT-3 and 5′-CTGTGAAAGACACAGAACAGTACAGGGT-3′; G3PDH 5′-GACCCCTTCATTGACCTCAAC-3′ and 5′-GATGACCTTGCCCACAGCCTT-3′. Each amplification cycle consisted of 0.5 min at 94 °C for denaturation, 0.5 min at 55 °C for primer annealing, and 1 min at 72 °C for extension. In all of the amplification procedures, reverse transcriptase-free control assays consisting of the amplification mixture, the RNA sample, and distilled water in place of reverse transcriptase were used to check for possible contamination of the RNA samples with DNA. After PCR amplification, the fragments were stained with ethidium bromide and analyzed by agarose gel electrophoresis.

Statistics. All data were expressed as the mean value ± standard error of the mean (SEM). Three to four samples were analyzed in each experiment. Comparisons were subjected to one-way analysis of variance followed by Fisher's least significant difference test. Significance was accepted at $P < 0.05$.

RESULTS AND DISCUSSION

MAG Induces G0/G1 Cell Cycle Arrest in Human U373 Cells. To study the effect of MAG on cell growth rate, U373 cells were cultured for 6 days without or with MAG (0−40 μM), and the cells were then harvested and counted. As shown in **Figure 1a**, MAG (0−40 μM) induced a concentration-dependent inhibition of growth in human U373 cells. To confirm that the MAG-induced decrease in cell number of U373 cells was not due to cell death, we conducted a viability assay by treating the cells with U373 cells for 3 or 6 days at the concentrations (5−40 μM) used in the study of cell growth inhibition. Trypan blue exclusion assays indicated that there was no significant difference in cell viability between control and MAG-treated U373 cells (**Figure 1b**), suggesting that there was an inhibitory effect of MAG on the mechanisms for cell division in the subcultured U373 cells. To further examine the actions of MAG on cell cycle regulatory mechanisms, the U373 cells were switched to media with 0.04% FBS for 24 h to render them quiescent and to synchronize their mitotic activities at the G0/G1 phase. The synchronized cells were then returned to culture media supplemented with 10% FBS,

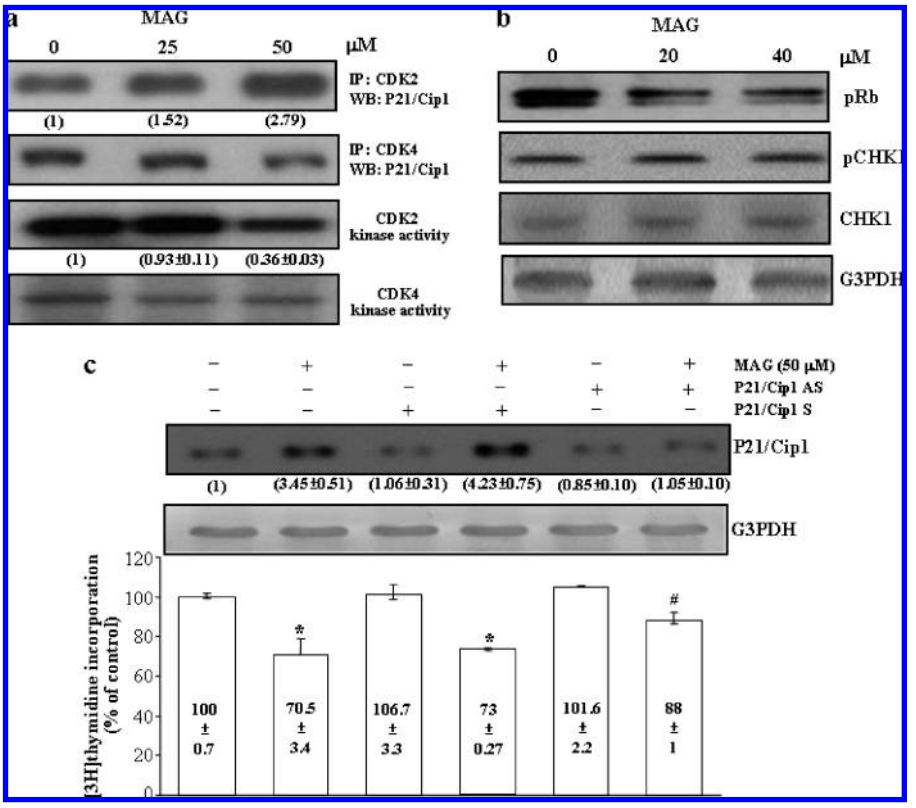

Figure 3. Involvement of p21/Cip1 in the MAG-induced decrease of thymidine incorporation in U373 cells. (**a**) MAG increased the formation of CDK2-p21/Cip1, but not CDK4-p21/Cip1, complex in U373 cells. The CDK2, but not CDK4, activity was decreased by MAG. Results from a representative experiment are shown. Values shown in parentheses represent the formation of the CDK2-p21/Cip1 complex. The CDK2 and CDK4 kinase activities were determined as described in the Materials and Methods. Results from a representative experiment are shown. Values (means ± SEM; $n = 3$) shown in parentheses represent the kinase activity of CDK2. WB, Western blot analysis. (**b**) MAG decreased the levels of phosporylated Rb (pRb) but not phosphorylated CHK1 (pCHK1) and total CHK1 protein. Results from a representative experiment are shown. The membrane was probed with anti-G3PHD antibody to verify equivalent protein loading. (**c**) Antisense p21/Cip1 oligonucleotide (AS) was added to U373 cells at a final concentration of 20 nM at 16 h before the cell was challenged with 10% FBS and 50 μM MAG for an additional 21 h. Pretreatment of U373 cells with AS p21/Cip1, but not S p21/Cip1, prevented the MAG-induced increase of p21/Cip1 protein level (top panel: Results from a representative experiment are shown. Values shown in parentheses represent the means ± SEM of p21/Cip1 protein levels from three experiments) and decrease of [^{3}H]thymidine incorporation (bottom panel: Values represent the means ± SEM; $n = 4$). *$p < 0.05$ vs control. $^{\#}p < 0.05$ vs 50 μM MAG-treated. AS, antisense oligonucleotide; and S, sense oligonucleotide.

and at various times thereafter, they were harvested for [^{3}H]thymidine incorporation and flow cytometric analyses. As illustrated in **Figure 1c**, MAG (50 μM) treatment caused a reduction of thymidine incorporation into U373 cells during the S phase of the cell cycle. **Figure 1d** shows that MAG induced a significant accumulation of cells in the G0/G1 phase of the cell cycle, suggesting that the observed growth inhibitory effect of MAG in the U373 was due to an arrest of DNA replication at the G0/G1 of the cell cycle.

Alterations in Cell Cycle Activity. To investigate the molecular mechanisms underlying MAG-induced G0/G1 arrest, the cells were switched to media with 0.04% FBS for 24 h to render them quiescent at the G0/G1 phase. The cells were then returned to culture media supplemented with 10% FBS and 0.05% DMSO without or with MAG (20−40 μM), and at 24 h thereafter, they were harvested for protein extraction and Western blot analyses to examine the effects of MAG on the expression of cell cycle regulatory proteins. It has been generally believed that progression of cell cycle activity is regulated by coordinated successive activation of certain CDKs, which occurs late in the G1 phase and is instrumental in the transition from the G1 to the S phase (*20*, *21*). This CDK activation is in turn modulated by association with a number of regulatory subunits called cyclins and with a group of CDK-inhibitory proteins designated CKIs (*22*). Cyclins have been identified as cyclins A, D1, D3, and E, whereas the most common CDKs are CDK2 and CDK4. As shown in **Figure 2a**, the protein levels of cyclins A and D1, but not cyclin D3, CDK2, and CDK4, were decreased in the MAG-treated U373 cells. Because the CDK activity can be controlled by a group of CKIs, we examined the protein levels of p21/Cip1 and p27/Kip1, two known CKIs, in the MAG-treated U373 cells. As shown in **Figure 2b**, the protein levels of p21/Cip1, but not p27/Kip1, were increased in the MAG-treated U373 cells as compared with the DMSO-treated cells (control). The protein levels of p53 in U373 were not affected by the MAG treatment (**Figure 2b**). We also examined the change of the mRNA level of p21/Cip1 (**Figure 2c**) in the MAG-treated U373 cells. As illustrated in **Figure 2c**, MAG (20−40 μM) concentration dependently increased the levels of p21/Cip1 mRNA.

Previous studies have demonstrated that p21/Cip1 arrests the cell cycle at the G0/G1 phase through binding and inactivating the CDKs (*20*, *21*, *23*). In accord with the established notion that p21/Cip1 is a CDK inhibitor, we found that the formation of the p21/Cip1-CDK2 complex was increased and the assayable CDK2 activity was decreased in the MAG-treated U373 cells (**Figure 3a**). In contrast, the formation of p21/Cip1-CDK4 complex and the CDK4 activity were not significantly changed (if there is any change). We further examined the levels of pRb protein, which can bind to the E2F-1 transcription factor and prevent it from interacting with the cells transcription machinery. As shown in

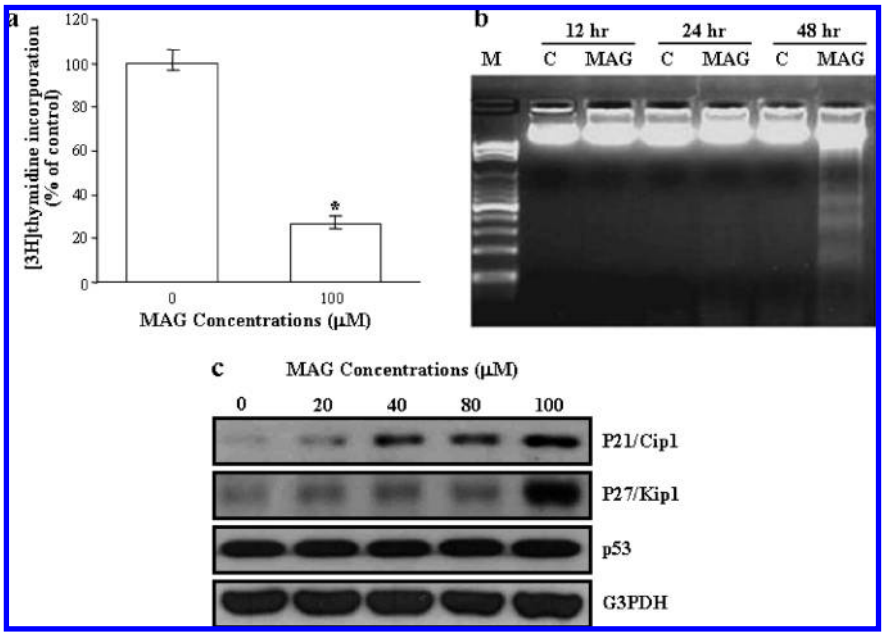

Figure 4. MAG induces DNA fragmentation in U373. (**a**) MAG at a concentration of 100 μM induced a dramatic decrease of [^{3}H]thymidine incorporation in U373 cells. Values represent the means ± SEM (n = 4). *p < 0.05 vs control. (**b**) A typical DNA ladder pattern associated with apoptosis was observed in U373 cells treated with 100 μM MAG for 48 h. (**c**) MAG (0−100 μM) concentration dependently increased the protein levels of p21/Cip1 but not p53. The levels of p27/Kip1 protein in U373 were not changed significantly by MAG at lower concentrations (0−80 μM) but were increased dramatically at a higher concentration (100 μM).

Figure 3b, MAG treatment decreased the levels of phosphorylated Rb protein.

It has been indicated that the G2/M cell cycle checkpoint is tightly regulated by the Cdc2/Cyclin B, which is required for entry into mitosis (*24*). In the MAG-treated U373 cells, the level of cyclin B protein was not changed significantly (**Figure 2a**). Moreover, MAG treatment did not cause any significant change of the levels of Wee1 and CDC25C protein, two major CDC2 activity regulators, and of CHK1 protein, which is essential for the G2/M DNA damage-induced checkpoint (**Figure 3b**). Taken together, these data suggest that MAG arrested the U373 cells at the G0/G1, but not G2/M, phase of the cell cycle.

A number of studies have suggested that p21/Cip1 does have tumor suppressor properties in human glioblastoma due to its high expression level found in several human brain tumors (*22*, *25*). Replication-deficient adenovirus was utilized as an expression vector to transfer exogenous p53 and p21/Cip1 cDNAs into the U373 glioma cells and demonstrated that overexpression of p21/Cip1 induced a cell cycle arrest but did not induce apoptosis (*26*), suggesting that p21/Cip1 might protect the cells from p53-mediated programmed cell death. To further demonstrate that the increased p21/Cip1 expression observed in the MAG-treated U373 correlated with G0/G1 arrest, the experiment illustrated in **Figure 3c** was carried out. As shown in **Figure 3c**, MAG treatment increased the p21/Cip1 protein levels and decreased the [^{3}H]thymidine incorporation in U373 cells. However, treatment of the cells with a p21/Cip1 antisense oligonucleotide, which blocked the p21/Cip1 induction, prevented the MAG-induced decrease of [^{3}H]thymidine incorporation. In contrast, a p21/Cip1 sense oligonucleotide, which did not affect the expression of p21/Cip1, failed to prevent the MAG-induced decrease of [^{3}H]thymidine incorporation. Accordingly, we concluded that MAG induced an increase in p21/Cip1 expression, which in turn inhibited the CDK2 enzyme activities and led to the impairment of U373 in the transition from the G1 to the S phase.

Previously, we demonstrated that MAG inhibited proliferation of liver and colon cancer cell lines with p53 wild-type (Hep-G2 and COLO-205) or mutated (Hep-3B and HT-29), suggesting that p53 is not required for the MAG-induced proliferation inhibition in cancer cell lines (*10*). Although p21/Cip1 has been recognized to be a critical downstream effector of p53 protein, some studies have shown that p21/Cip1 can also be induced through a p53-independent pathway (*27*). The p53 gene in U373 cell line has a point mutation at codon 273 (CGT→ CAT). This mutation leads to replacement of an arginine by a histidine at codon 273 on exon 5. In the present study, a high basal level of p53 protein was detected in the untreated U373 cells. MAG at a range of concentrations (0−100 μM) did not increase the level of p53 protein (**Figures 2b** and **4c**), suggesting that p53 might not be involved in the MAG-induced proliferation inhibition and the occurrence of apoptosis in U373. Instead, our data indicate that the induction of p21/Cip1 expression might contribute to the MAG-induced proliferation inhibition in U373. Moreover, MAG increased p21/Cip1 at both mRNA and protein levels (**Figure 2b**,**c**). A similar result was demonstrated by a previous study from another group showing that hypoxia increased the level of p21 protein, but not p53 protein, in U373 cells (*28*).

Effect of MAG on DNA Fragmentation and CKI Protein Levels of U373 Cells. We further examined the MAG effect on U373 cells when the concentration of MAG was increased. As illustrated in **Figure 4a**, the thymidine incorporation was dramatically decreased in the U373 cells treated with MAG at a concentration of 100 μM. **Figure 4b** shows that the DNA laddering effect was observed in U373 cells treated with MAG at a concentration of 100 μM for 48 h. We also examined the CKI protein levels in U373 treated with higher concentrations of MAG. As illustrated in **Figure 4c**, MAG at a range of concentrations (0−100 μM) concentration dependently increased the levels of p21. However, the levels of p27 protein were not changed significantly at lower concentrations of MAG (0−80 μM) but were dramatically increased when the MAG concentration reached 100 μM. In contrast, the levels of p53 protein were not changed significantly by MAG treatment even at a concentration of 100 μM. It seems that the induction of p27/Kip1 protein was correlated with the

occurrence of apoptosis in U373 cells. Recently, it has been shown that overexpression of p27/Kip1 induces apoptosis and inhibits tumor formation in vitro and in vitro (*29*). Moreover, cotransduction of p27/Kip1 strongly augments Fas ligand- and caspase-8-mediated apoptosis in U-373 (*30*). The dramatically increased p27/Kip protein levels were observed in the U373 treated with a higher concentration (100 μM) of MAG but not lower concentrations ($\leq$40 μM), suggesting that the p27/Kip1 protein might be involved in the MAG-induced apoptosis but not cell growth arrest.

In conclusion, multifocal glioblastomas constitute an increasingly diagnosed subgroup of glioblastoma multiforme, the most malignant primary brain tumor in adults. Because glioblastoma multiforme is resistant to all currently used treatments, to search for new therapeutic strategies is urgent. The current experimental models used in discovering new antiglioma therapies include either murine gliomas (*31*), which have biologic characteristics that are very different from those of human gliomas, or human glioma cell lines grafted subcutaneously onto the flanks of immunodeficient mice (*14*, *16*, *32*). However, in such models, diffuse invasiveness into the brain parenchyma, the hallmark of the malignant human glioma phenotype, is no longer valid. Migrating glioma cells are known to escape from chemotherapeutic agent-induced apoptosis and thus the compounds that restore the apoptosis-resistant cells not only delay the invasion of cancer cells into brain parenchyma but also enhance the sensitivity of these slowly migrating cells (*33*). The pharmacokinetics of MAG in rats demonstrated that MAG can cross the blood−brain barrier (BBB), and there is no significant difference among various regions of the brain after 10 min of MAG (5 mg/kg, i.v.) administration; the mean concentration of MAG in the brain was approximately 4-fold as high as that in the plasma (*34*). Although the functional BBB has been identified for a long time, the complexity and relevance of the blood−brain−tumor barrier has been recognized recently as an important factor that limits the effective treatment of central nervous system neoplasms. A previous report has demonstrated that MAG could relieve the heatstroke-induced cerebral ischemic injury through inhibiting of free radical formation (*35*). This finding demonstrated again that MAG could cross the BBB and act in the brain. In this study, we observed that MAG suppresses proliferation of cultured human U373 cells by inhibiting DNA synthesis and activating apoptosis. Our study provides the basis of molecular mechanisms for MAG in brain cancer treatment. Taken together with previous studies, our present study suggested that use of MAG in the treatment of glioblastoma showed several advantages that included (1) increased the occurrence of apoptosis, (2) induced the cell cycle arrest, and (3) crossed the BBB. The universality of MAG in the inhibition of cancer cell proliferation would make it a very attractive agent for cancer chemotherapy.

ABBREVIATIONS USED

BBB, blood−brain barrier; CDK, cyclin-dependent kinase; CDKIs, cyclin-dependent kinase inhibitors; DMSO, dimethyl sulfoxide; FBS, fetal bovine serum; IP, immunoprecipitation; MAG, magnolol; SDS-PAGE, sodium dodecyl sulfate−polyacrylamide gel electrophoresis.

LITERATURE CITED

(1) Surawicz, T. S.; Davis, F.; Freels, S.; Laws, E. R., Jr.; Menck, H. R. Brain tumor survival: Results from the National Cancer Data Base. *J. Neuro-Oncol.* **1998**, *40* (2), 151–160.

(2) Cairncross, J. G.; Ueki, K.; Zlatescu, M. C.; Lisle, D. K.; Finkelstein, D. M.; Hammond, R. R.; Silver, J. S.; Stark, P. C.; Macdonald, D. R.; Ino, Y.; Ramsay, D. A.; Louis, D. N. Specific genetic predictors of chemotherapeutic response and survival in patients with anaplastic oligodendrogliomas. *J. Natl. Cancer Inst.* **1998**, *90* (19), 1473–1479.

(3) Heiss, W. D.; Turnheim, M.; Mamoli, B. Combination chemotherapy of malignant glioma. Effect of postoperative treatment with CCNU, vincristine, amethopterine and procarbazine. *Eur. J. Cancer* **1978**, *14* (11), 1191–1202.

(4) Kesari, S.; Schiff, D.; Drappatz, J.; LaFrankie, D.; Doherty, L.; Macklin, E. A.; Muzikansky, A.; Santagata, S.; Ligon, K. L.; Norden, A. D.; Ciampa, A.; Bradshaw, J.; Levy, B.; Radakovic, G.; Ramakrishna, N.; Black, P. M.; Wen, P. Y. Phase II study of protracted daily temozolomide for low-grade gliomas in adults. *Clin. Cancer Res.* **2009**, *15* (1), 330–337.

(5) Postma, T. J.; van Groeningen, C. J.; Witjes, R. J.; Weerts, J. G.; Kralendonk, J. H.; Heimans, J. J. Neurotoxicity of combination chemotherapy with procarbazine, CCNU and vincristine (PCV) for recurrent glioma. *J. Neuro-Oncol.* **1998**, *38* (1), 69–75.

(6) Neyns, B.; Sadones, J.; Chaskis, C.; De Ridder, M.; Keyaerts, M.; In'T Veld, P.; Michotte, A. The role of chemotherapy in the treatment of low-grade glioma—A review of the literature. *Acta Neurol. Belg.* **2005**, *105* (3), 137–143.

(7) Perilongo, G. Considerations on the role of chemotherapy and modern radiotherapy in the treatment of childhood low grade glioma. *J. Neuro-Oncol.* **2005**, *75* (3), 301–307.

(8) Fujita, M.; Itokawa, H.; Sashida, Y. Studies on the components of Magnolia obovata Thunb. II. On the components of the methanol extract of the bark. *Yakugaku Zasshi* **1973**, *93* (4), 422–428.

(9) Lee, D. H.; Szczepanski, M. J.; Lee, Y. J. Magnolol induces apoptosis via inhibiting the EGFR/PI3K/Akt signaling pathway in human prostate cancer cells. *J. Cell Biochem.* **2009**, *106* (6), 1113–1122.

(10) Lin, S. Y.; Liu, J. D.; Chang, H. C.; Yeh, S. D.; Lin, C. H.; Lee, W. S. Magnolol suppresses proliferation of cultured human colon and liver cancer cells by inhibiting DNA synthesis and activating apoptosis. *J. Cell Biochem.* **2002**, *84* (3), 532–544.

(11) Yang, S. E.; Hsieh, M. T.; Tsai, T. H.; Hsu, S. L. Effector mechanism of magnolol-induced apoptosis in human lung squamous carcinoma CH27 cells. *Br. J. Pharmacol.* **2003**, *138* (1), 193–201.

(12) Ikeda, K.; Sakai, Y.; Nagase, H. Inhibitory effect of magnolol on tumour metastasis in mice. *Phytother. Res.* **2003**, *17* (8), 933–937.

(13) Ho, Y. S.; Lee, H. M.; Mou, T. C.; Wang, Y. J.; Lin, J. K. Suppression of nitric oxide-induced apoptosis by N-acetyl-L-cysteine through modulation of glutathione, bcl-2, and bax protein levels. *Mol. Carcinog.* **1997**, *19* (2), 101–113.

(14) Arai, T.; Joki, T.; Akiyama, M.; Agawa, M.; Mori, Y.; Yoshioka, H.; Abe, T. Novel drug delivery system using thermoreversible gelation polymer for malignant glioma. *J. Neuro-Oncol.* **2006**, *77* (1), 9–15.

(15) Lee, W. S.; Chen, R. J.; Wang, Y. J.; Tseng, H.; Jeng, J. H.; Lin, S. Y.; Liang, Y. C.; Chen, C. H.; Lin, C. H.; Lin, J. K.; Ho, P. Y.; Chu, J. S.; Ho, W. L.; Chen, L. C.; Ho, Y. S. In vitro and in vivo studies of the anticancer action of terbinafine in human cancer cell lines: G0/G1 p53-associated cell cycle arrest. *Int. J. Cancer* **2003**, *106* (1), 125–137.

(16) Kim, K. J.; Wang, L.; Su, Y. C.; Gillespie, G. Y.; Salhotra, A.; Lal, B.; Laterra, J. Systemic anti-hepatocyte growth factor monoclonal antibody therapy induces the regression of intracranial glioma xenografts. *Clin. Cancer Res.* **2006**, *12* (4), 1292–1298.

(17) Chen, R. J.; Lee, W. S.; Liang, Y. C.; Lin, J. K.; Wang, Y. J.; Lin, C. H.; Hsieh, J. Y.; Chaing, C. C.; Ho, Y. S. Ketoconazole induces G0/G1 arrest in human colorectal and hepatocellular carcinoma cell lines. *Toxicol. Appl. Pharmacol.* **2000**, *169* (2), 132–141.

(18) Aoki, S.; Kong, D.; Suna, H.; Sowa, Y.; Sakai, T.; Setiawan, A.; Kobayashi, M. Aaptamine, a spongean alkaloid, activates p21 promoter in a p53-independent manner. *Biochem. Biophys. Res. Commun.* **2006**, *342* (1), 101–106.

(19) Suzui, M.; Masuda, M.; Lim, J. T.; Albanese, C.; Pestell, R. G.; Weinstein, I. B. Growth inhibition of human hepatoma cells by acyclic retinoid is associated with induction of p21(CIP1) and inhibition of expression of cyclin D1. *Cancer Res.* **2002**, *62* (14), 3997–4006.

(20) Yu, D. H.; Macdonald, J.; Josephs, S.; Liu, Q.; Nguy, V.; Tor, Y.; Wong-Staal, F.; Li, Q. X. MDDD, a 4,9-diazapyrenium derivative, is selectively toxic to glioma cells by inducing growth arrest at G0/G1 independently of p53. *Invest. New Drugs* **2006**, *24* (6), 489–498.
(21) Komata, T.; Kanzawa, T.; Takeuchi, H.; Germano, I. M.; Schreiber, M.; Kondo, Y.; Kondo, S. Antitumour effect of cyclin-dependent kinase inhibitors (p16(INK4A), p18(INK4C), p19(INK4D), p21-(WAF1/CIP1) and p27(KIP1)) on malignant glioma cells. *Br. J. Cancer* **2003**, *88* (8), 1277–1280.
(22) Krex, D.; Mohr, B.; Appelt, H.; Schackert, H. K.; Schackert, G. Genetic analysis of a multifocal glioblastoma multiforme: A suitable tool to gain new aspects in glioma development. *Neurosurgery* **2003**, *53* (6), 1377−1384; discussion 1384.
(23) Harmalkar, M. N.; Shirsat, N. V. Staurosporine-induced growth inhibition of glioma cells is accompanied by altered expression of cyclins, CDKs and CDK inhibitors. *Neurochem. Res.* **2006**, *31*, 685–692.
(24) Huang, T. S.; Shu, C. H.; Chao, Y.; Chen, S. N.; Chen, L. L. Activation of MAD 2 checkprotein and persistence of cyclin B1/CDC 2 activity associate with paclitaxel-induced apoptosis in human nasopharyngeal carcinoma cells. *Apoptosis* **2000**, *5* (3), 235–241.
(25) Begnami, M. D.; Rushing, E. J.; Evangelista, R.; Santi, M.; Quezado, M. Evaluation of RB gene and cyclin-dependent kinase inhibitors P21 and P27 in pleomorphic xantoastrocytoma. *Int. J. Surg. Pathol.* **2006**, *14* (2), 113–118.
(26) Gomez-Manzano, C.; Fueyo, J.; Kyritsis, A. P.; McDonnell, T. J.; Steck, P. A.; Levin, V. A.; Yung, W. K. Characterization of p53 and p21 functional interactions in glioma cells en route to apoptosis. *J. Natl. Cancer Inst.* **1997**, *89* (14), 1036–1044.
(27) Michiell, P.; Chedid, M.; Lin, D.; Pierce, J. H.; Mercer, W. E.; Givol, D. Induction of WAF1/CIP1 by a p53-independent pathway. *Cancer Res.* **1994**, *54* (13), 3391–3395.
(28) Bell, H. S.; Whittle, I. R.; Bader, S. A.; Wharton, S. B. Discovery of a perinecrotic 60 kDa MDM2 isoform within glioma spheroids and glioblastoma biopsy material. *Neuropathol. Appl. Neurobiol.* **2005**, *31* (2), 191–202.
(29) Wang, X.; Gorospe, M.; Huang, Y.; Holbrook, N. J. p27Kip1 overexpression causes apoptotic death of mammalian cells. *Oncogene* **1997**, *15* (24), 2991–2997.
(30) Shinoura, N.; Furitsu, T.; Asai, A.; Kirino, T.; Hamada, H. Co-transduction of p27Kip1 strongly augments Fas ligand- and caspase-8-mediated apoptosis in U-373MG glioma cells. *Anticancer Res.* **2001**, *21* (5), 3261–3268.
(31) Ahmadi, R.; Urig, S.; Hartmann, M.; Helmke, B. M.; Koncarevic, S.; Allenberger, B.; Kienhoefer, C.; Neher, M.; Steiner, H. H.; Unterberg, A.; Herold-Mende, C.; Becker, K. Antiglioma activity of 2,2′:6′,2″-terpyridineplatinum(II) complexes in a rat model—Effects on cellular redox metabolism. *Free Radical Biol. Med.* **2006**, *40* (5), 763–778.
(32) Koller, E.; Propp, S.; Zhang, H.; Zhao, C.; Xiao, X.; Chang, M.; Hirsch, S. A.; Shepard, P. J.; Koo, S.; Murphy, C.; Glazer, R. I.; Dean, N. M. Use of a chemically modified antisense oligonucleotide library to identify and validate Eg5 (kinesin-like 1) as a target for antineoplastic drug development. *Cancer Res.* **2006**, *66* (4), 2059–2066.
(33) Manero, F.; Gautier, F.; Gallenne, T.; Cauquil, N.; Gree, D.; Cartron, P. F.; Geneste, O.; Gree, R.; Vallette, F. M.; Juin, P. The small organic compound HA14−1 prevents Bcl-2 interaction with Bax to sensitize malignant glioma cells to induction of cell death. *Cancer Res.* **2006**, *66* (5), 2757–2764.
(34) Tsai, T. H.; Chou, C. J.; Chen, C. F. Pharmacokinetics and brain distribution of magnolol in the rat after intravenous bolus injection. *J. Pharm. Pharmacol.* **1996**, *48* (1), 57–59.
(35) Chang, C. P.; Hsu, Y. C.; Lin, M. T. Magnolol protects against cerebral ischaemic injury of rat heatstroke. *Clin. Exp. Pharmacol. Physiol.* **2003**, *30* (5−6), 387–392.

Received May 4, 2009. Revised manuscript received July 20, 2009. Accepted July 21, 2009. This research was supported by a grant from the National Science Council of the Republic of China (NSC96-2320-B-038-023) to W.-S.L.